Proceedings of the ASME 2010 International Mechanical Engineering Congress & Exposition
IMECE2010
November 12-18, 2010, Vancouver, British Columbia, Canada

IMECE2010-39672

Numerical Analysis of Liquid Water Droplets Removal in Gas Channels of a PEM Fuel Cell

Chin-Hsiang Cheng
Department of Aeronautics and Astronautics
National Cheng-Kung University
Tainan, Taiwan

Wei-Shan Han
Department of Aeronautics and Astronautics
National Cheng-Kung University
Tainan, Taiwan

Chun-I Lee
Green Energy and Environment Research Lab., Industrial Technology Research Institute, Taiwan

Huan-Ruei Shiu
Green Energy and Environment Research Lab., Industrial Technology Research Institute, Taiwan

Ssu-Tai Lin
Green Energy and Environment Research Lab., Industrial Technology Research Institute, Taiwan

ABSTRACT

The present study is concerned with the dynamic behavior of the liquid water droplets in the water removal process in the serpentine channels of a PEM fuel cell based on computational fluid dynamic (CFD) simulation. The volume of fluid (VOF) model is adopted to trace the interface between the liquid and the gas phases such that the motion of the liquid droplets can be observed. Effects of the incoming velocity are evaluated. In addition, the surface hydrophobic properties are influential to the droplets motion; therefore, the contact angle of the liquid droplet attached on the channel wall has been varied. In addition, the orientation of the bipolar plate is regarded as another important parameter in the present study. Results show that among these parameters considered, the incoming flow velocity and the contact angle are two key parameters which greatly affect the dynamic behavior of the liquid droplets. The liquid droplets attached on the wall of the bipolar plate can be removed by the gas flow only when the contact angle or the incoming flow velocity is sufficiently high.

Keywords: Fuel cell; Water management; Liquid droplet; Contact angle; VOF

INTRODUCTION

In a proton exchange membrane (PEM) fuel cell, the direct conversion of chemical energy of the gas reactants to electrical energy is achieved with high efficiency and good environmental compatibility. However, the performance of the contemporary PEM fuel cell still needs to be significantly improved toward engineering optimization and cost reduction [1-4].

Water management in a PEM fuel cell has been one of the critical challenging issues. In practices, the water vapor in the fuel cells is produced from the electrochemical reaction taking place in the catalyst layer on the cathode side, it penetrate through the gas diffusion layer and condenses on the walls of the gas channel on the bipolar plate if the partial pressure of the water vapor exceeds the saturation pressure or when the operating temperature of a PEM fuel cell is lower than the dew point temperature of the gas mixture. Besides, additional water may be supplied by an external humidifier which is used to add moisture into the hydrogen gas on the anode side so as to optimize the hydration of the proton exchange membrane. When the water vapor or the liquid droplets are not able to be readily removed from the channels by the gas flow, the liquid water condensate may be accumulated to cause water flooding and retard the mass transport by occupying the pores of the gas diffusion and catalyst layers. Therefore, maintaining the proper balance in fuel cell between water production and removal is important in improving the PEM fuel cell performance. Thus, water management has become a critical issue for fuel cell design [5-7].

In an earlier study, Fuller and Newman [8] performed a numerical simulation of the effect of water vapor at the different flow rates in the flow channels. Kimble and Vanderborgh [9] presented a numerical model which was used to study the effect of liquid water formed at different reactant concentrations along the flow channels. Quan, et al.[10] built a serpentine-channel experimental module to investigate the dynamic behavior of the liquid water droplets with different initial velocity distribution as the inlet flow rate was fixed.

In a recent experimental study performed by the present group of authors, it is found that the contact angle (α) of the liquid water droplets attached on the channel wall of a metallic bipolar plate can be greatly altered by coating a microscale carbon thin film on the wall (Fig.1). The thin-film coating changes the surface hydrophobic properties and the contact angle, which are critical to the static and dynamic behavior of the liquid droplets. To yield a further understanding of the dynamic behavior of the liquid water droplets in the water

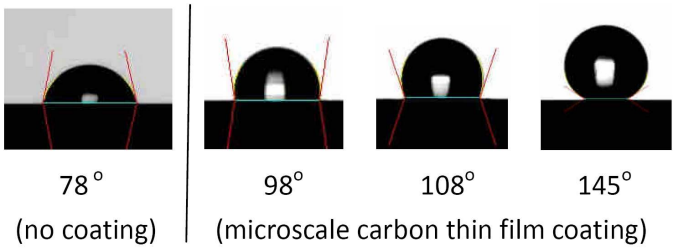

Figure 1 Contact angle changed by carbon thin-film coating.

removal process, in this study a numerical simulation based on computational fluid dynamic analysis has been performed. The volume of fluid (VOF) model is adopted to trace the interface between the liquid and the gas phases such that the motion of the liquid droplets can be predicted. To extensively investigate the effects of the contact angle on the droplet behavior, the contact angle is varied from 60° to 170°. In addition, the effects of the incoming air velocity and the orientation of the bipolar plate are also regarded as important parameter in the present study.

NOMENCLATURE

f_σ	surface tension force (N)
P	pressure (N/m^2)
u, v, w	velocity components (m/s)
V	incoming air velocity (m/s)
g	gravitational acceleration (m/s^2)
t	time (s)
x, *y*, *z*	rectangular coordinates
$\vec{n}$	normal vector of liquid surface

Greek symbols

α	contact angle (degree)
σ	surface tension coefficient (N/m)
ρ	fluid density (kg m^{-3})
μ	viscosity coefficient (kg/m-s)
κ	curve curvature

THEORETICAL ANALYSIS

Figure 2 shows the dimensions of the gas flow channel and the initial conditions. The U-shaped channel is 1 mm wide, 1 mm deep, and totally 25 mm long, which is a part of serpentine channel. Initially, a static liquid droplet, of 0.3 mm radius and with specified contact angle, is placed on the channel wall. The distance from the inlet to the center of the liquid droplet is 5 mm. The air then enters the U-shaped channel at constant velocity and exits from the outlet. It is desired that the liquid droplet can be washed away by the air flow. In theory, the dynamic behavior of the liquid droplet is also influenced by the surface tension and the viscosity of the liquid. For liquid water, the surface tension and the dynamic viscosity are set to be 0.072 N/m and 8.90×10^{-4} Pa·s, respectively.

The theoretical model is developed based on the following assumptions:

(1) The gas flow is assumed to be incompressible and laminar.
(2) The influence of gravity on the motion of the droplet and the gas flow is considered and the gravity direction is changed in terms of the orientation of the bipolar plate.
(3) The thermodynamic and the transport properties of the air and the liquid are all constant.
(4) The flow is isothermal without neither condensation nor vaporization.

The governing equations for the present study are expressed in the following:

Mass conservation equation:

$$\frac{\partial \rho}{\partial t}+\rho\frac{\partial u}{\partial x}+\rho\frac{\partial v}{\partial y}+\rho\frac{\partial w}{\partial z}=0 \qquad (1)$$

where *u*, *v*, *w* is the velocity components in x-, y-, and z-direction, respectively.

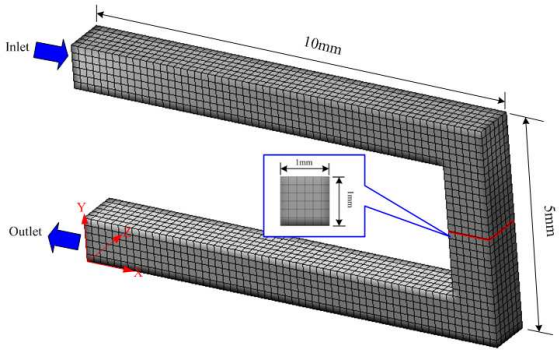

(a) Dimensions of the gas flow channel.

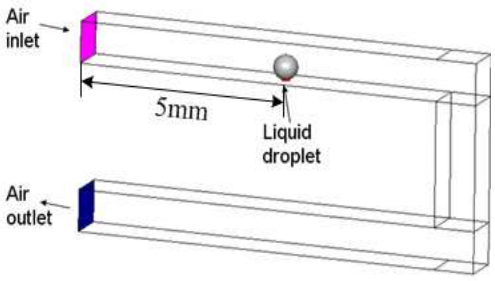

(b) Initial position of liquid water droplet.

Figure 2 Schematics of the numerical module.

Momentum conservation equation:

$$\frac{\partial(\rho u)}{\partial t}+u\frac{\partial(\rho u)}{\partial x}+v\frac{\partial(\rho u)}{\partial y}+w\frac{\partial(\rho u)}{\partial z} = -\frac{\partial P}{\partial x}+\mu\left(\frac{\partial^2 u}{\partial x^2}+\frac{\partial^2 u}{\partial y^2}+\frac{\partial^2 u}{\partial z^2}\right)+\rho g_x+f_{\sigma x} \quad (2)$$

$$\frac{\partial(\rho v)}{\partial t}+u\frac{\partial(\rho v)}{\partial x}+v\frac{\partial(\rho v)}{\partial y}+w\frac{\partial(\rho v)}{\partial z} = -\frac{\partial P}{\partial y}+\mu\left(\frac{\partial^2 v}{\partial x^2}+\frac{\partial^2 v}{\partial y^2}+\frac{\partial^2 v}{\partial z^2}\right)+\rho g_y+f_{\sigma y} \quad (3)$$

$$\frac{\partial(\rho w)}{\partial t}+u\frac{\partial(\rho w)}{\partial x}+v\frac{\partial(\rho w)}{\partial y}+w\frac{\partial(\rho w)}{\partial z} = -\frac{\partial P}{\partial z}+\mu\left(\frac{\partial^2 w}{\partial x^2}+\frac{\partial^2 w}{\partial y^2}+\frac{\partial^2 w}{\partial z^2}\right)+\rho g_z+f_{\sigma z} \quad (4)$$

where ρ is the fluid density, u, v and w are the incoming air velocity in different direction, P the pressure, μ is the viscosity coefficient, g the gravitational acceleration and f_σ is the surface tension.

Surface tension equation:

$$f_\sigma = \nabla P = \Delta P\vec{n} = \sigma\kappa\nabla\alpha = -\sigma\,\nabla\left(\frac{\nabla\alpha}{|\nabla\alpha|}\right)\nabla\alpha \quad (5)$$

where

$$k = -\left(\nabla\bullet\,\vec{n}\right) \quad (6)$$

$$\hat{n} = \frac{\vec{n}}{|\vec{n}|} \quad (7)$$

and σ is the surface tension coefficient.

Volume of fraction (VOF) equation:

$$\frac{\partial F}{\partial t}+u\frac{\partial F}{\partial x}+v\frac{\partial F}{\partial y}+w\frac{\partial F}{\partial z}=0 \quad (8)$$

The value of volume fraction (F) can be determined as follows

$$F=\frac{\text{volume of fluid 1}}{\text{Total Volume of Cell volume}} \quad (9)$$

The entire computational domain can be divided into three regions by the volume fraction as

$$F=\begin{cases}1 \text{ for cell full of fluid2}\\ 0 \text{ for cell full of fluid1}\\ 0<F<1 \text{ for cell mixed with fluid1 and fluid2}\end{cases}$$

For each cell, the effective density and viscosity of the fluid in the equations (1) and (2) are calculated in terms of the volume fraction as

$$\rho=\rho_1 F+\rho_2\left(1-F\right) \quad (10)$$

$$\mu=\mu_1 F+\mu_2\left(1-F\right) \quad (11)$$

where the subscripts 1 and 2 denote the two fluids, F is the volume fraction.

Boundary conditions

In this study, the temperature of the entire domain is maintained at 300 K. The wall is with a no-slip boundary condition for the velocity components. The incoming air velocity at the inlet is assigned with a constant value of interest whereas at the outlet the pressure is fixed at 101,325 Pa.

Numerical methods and numerical model

The computation is performed based on the framework of a commercial software package, CFD-ACE+, and the base-line simulation conditions are complied with typical fuel cell operating conditions. Firstly, a three-dimensional simulation model is built, and a structured multi-grid solver is chosen in computation with a convergence criterion of 1×10^{-6} for all quantities. The package is developed based on SIMPLEC algorithm and finite-volume method. A grid system of 404,248 grid cells is adopted over the computation domain. Before the grid system is chosen, a grid-independency check has been performed. In the check, five grid systems, 23,000, 94,208, 244,904, 404,248, and 621,000 cells, are tested. Since contact angle is the most important parameter, these grid system are used individually to generate a static liquid droplet with 170° contact angle on the wall, as show in Fig. 3. It is found that the system of 404,248 cells is able to generate a droplet shape which is nearly the same as that generated with 621,000 cells. Thus, computations 404,248 cells are performed on a personal computer with Intel Core™ 2 Quad 2.6G CPU. Typical required computation time for a single case is around 10 days to complete one case.

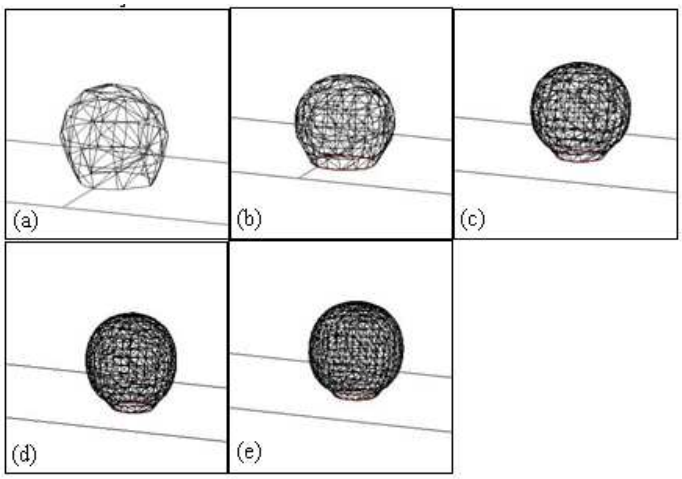

Figure 3 Grid independency check by generating a static liquid droplet with contact angle α=170°on the wall.
(a) 23,000 cells (b) 94,208 cells (c) 244,904 cells
(d) 404,248 cells (e) 621,000 cells

RESULTS AND DISCUSSION

Velocity and pressure fields

Figure 4 conveys the transient variation in the pressure distribution in the channel for the case at V=2 m/s and α=170°. The gravity direction is in the negative y-direction. In this figure, an appreciable pressure drop is observed over the liquid drop due to the sudden passage contraction caused by the existence of the liquid droplet. It is the difference in pressure between the front and the back of the liquid droplet that produces a form drag to remove the liquid droplet. The pressure difference increases with the size of the liquid droplet. It can be expected that when the channel is nearly blocked by the liquid droplet, the pressure difference reaches it maximum. The wetability of a liquid is defined in terms of the contact angle between a droplet of the liquid on the wall. It is observed that due to weaker wetability with a higher contact angle for the case shown in Fig.4, the droplet can be readily washed away from the channel by the air flow. During the removal process, the liquid droplet behaves like a flexible sphere as it collides with the walls of the channels. After the collision with the horizon bottom wall, the liquid droplet jumps up and then adheres to the opposing wall before exiting from the outlet. The reason how the liquid droplet is able to adhere to the wall opposing to the bottom wall is clarified in Figure 5. Figure 5 shows the snapshots of the streamlines of the air flow in the channel for the same case. It is interesting to notice that the air in the bottom right corner apparently goes upwards. With the help of the up-going flow, after the flexible liquid droplet rebounds off the bottom wall, the droplet is pushed up by the flow and then adheres to the opposing wall.

Effects of the incoming air velocity, the contact angle of the liquid droplet attached on the wall, and the orientation of the bipolar plate are regarded as influential parameters in the present study. The obtained results and discussion are given below.

Effects of incoming air velocity

Effects of incoming air velocity on the dynamic behavior of the liquid droplet with α=170° are plotted in Figure 6. The gravity direction is in the negative y-direction. The incoming air velocity is assigned to be 1, 2, 5, and 10 m/s. It is found that at α=170°, the liquid droplet can be removed by the air flow even at V=1 m/s. It is noticed that as $V \leq 5$ m/s, the liquid droplet maintains the shape of a sphere during the removal process. However, as V = 10 m/s, the droplet can be torn into smaller droplets by the shear stress produced by the air flow. The size of the smaller droplets is a function of the viscosity of the liquid and shear stress interaction between the liquid water and the air stream.

In general, the speed of water removal increases with the incoming air velocity as expected. A comparison in speed of water removal at various incoming air velocities is provided in Fig. 7 based on the snapshots at $t=1.5581\times10^{-2}$ sec. In this figure, three velocities are considered; e.g. V=1, 2, and 5 m/s. The gravity direction is still in the negative y-direction. It is clear that with V = 5 m/s, the removed liquid droplet can arrive at the exit in 1.5581×10^{-2} sec. However, at V = 1 m/s, the liquid droplet travels only a shorter distance (around 3 mm) from the initial position in the same period of time.

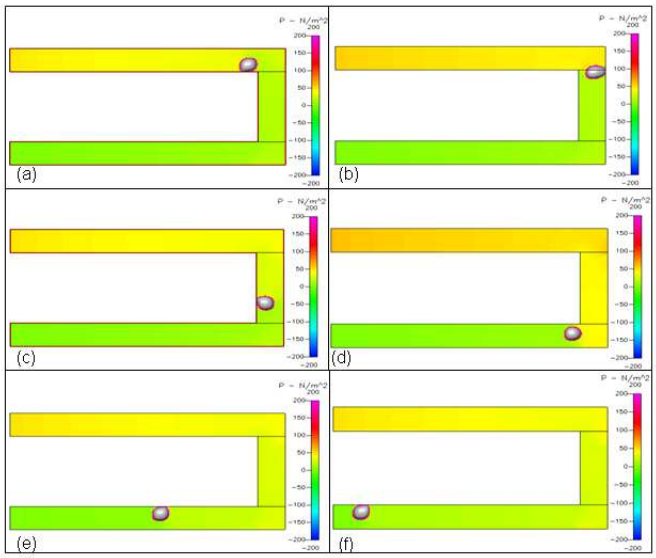

Figure 4 Snapshots of the pressure distribution in channel at V=2 m/s and α=170°. The gravity direction is in the negative y-direction. (a) 1.0221×10^{-2} sec (b) 1.3721×10^{-2} sec (c) 1.9071×10^{-2} sec (d) 2.3993×10^{-2} sec (e) 3.1105×10^{-2} sec (f) 3.6837×10^{-2} sec

Effects of orientation of the bipolar plate

When the orientation of the bipolar plate is changed, the direction of gravity in the numerical model is changed accordingly. In this study, five possible gravity directions are taken into consideration, including x-direction, negative x-direction, z-direction, y-direction, and negative y-direction. Plotted in Figure 8 is the dynamic behavior of liquid droplet under these different gravity directions at V=2 m/s and α=170°. It is noted that the influence of the gravity direction on the dynamic behavior of the liquid droplet is not appreciable. However, the speed of water removal may be affected by changing the gravity direction. For example, for this particular case shown in Fig.8, as the gravity direction is in the negative y-direction [Fig. 8(e)], it takes only about 3.82×10^{-2} s for the liquid droplet to be removed from the channel. As the gravity direction is set to be in the z-direction [Fig. 8(c)], it takes about 4.22×10^{-2} s. It is found that among the five gravity directions considered, the negative y-direction leads to a higher relative performance in liquid droplet removal.

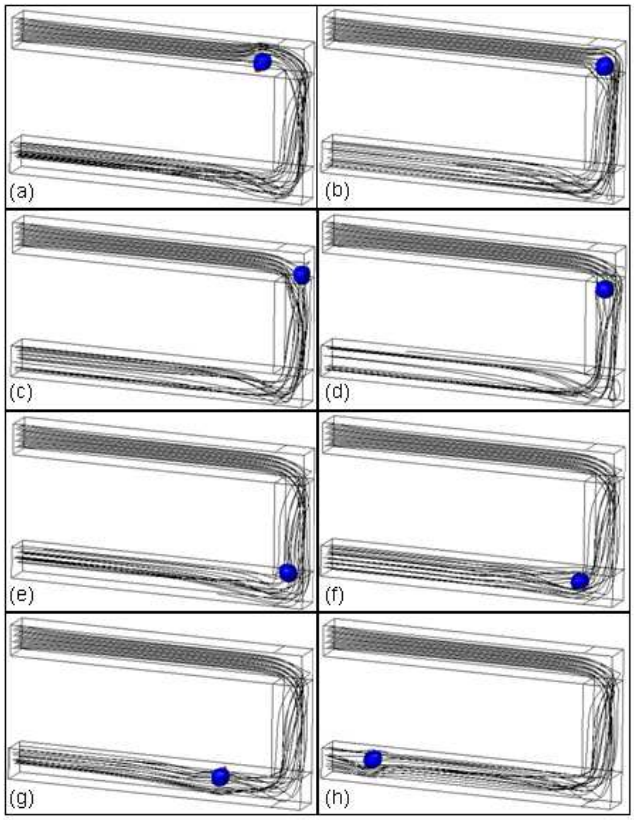

Figure 5 Snapshots of the streamlines of the air flow in channel at V=2 m/s and α=170°. The gravity direction is in the negative y-direction. (a) 9.722×10^{-3} sec (b) 1.1199×10^{-2} sec (c) 1.2243×10^{-2} sec (d) 1.4591×10^{-2} sec (e) 2.006×10^{-2} sec (f) 2.3742×10^{-2} sec (g) 2.77×10^{-2} sec (h) 3.6446×10^{-2} sec

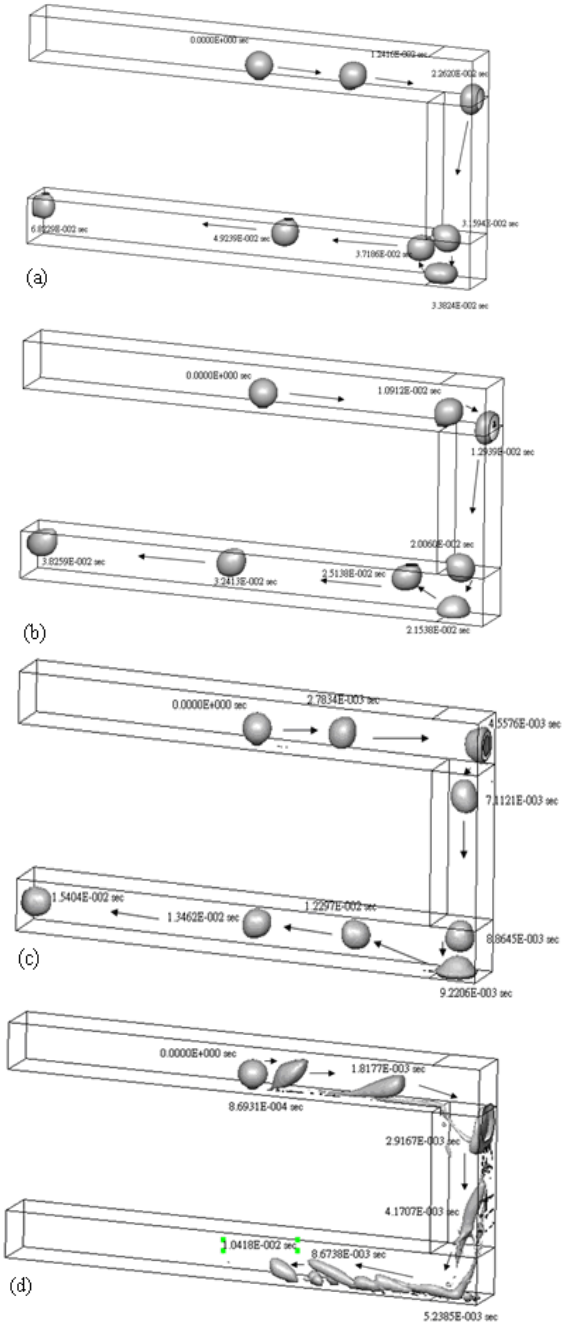

Figure 6 Effects of incoming air velocity on the dynamic behavior of liquid droplet at α=170°. The gravity direction is in the negative y-direction.
(a) V=1 m/s (b) V=2 m/s (c) V=5 m/s (d) V=10 m/s

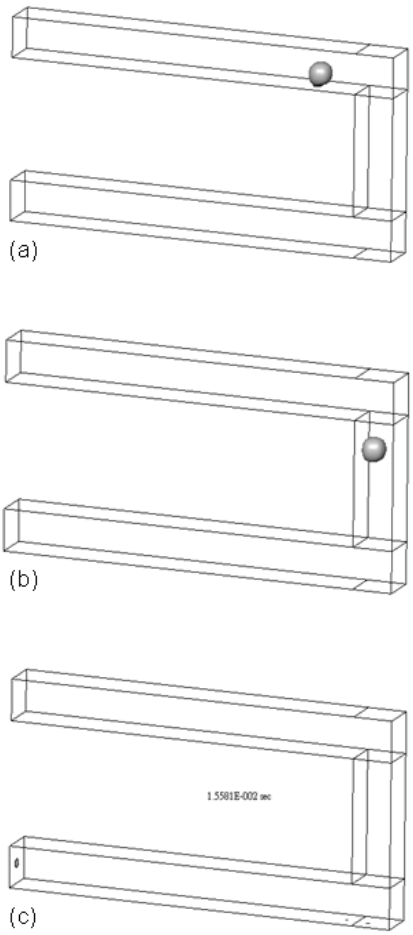

Figure 7 Comparison in speed of water removal based on the snapshots at $t=1.5581\times10^{-2}$ sec and $\alpha=170°$. The gravity direction is in the negative y-direction.
(a) V=1 m/s (b) V=2 m/s (c)V=5 m/s

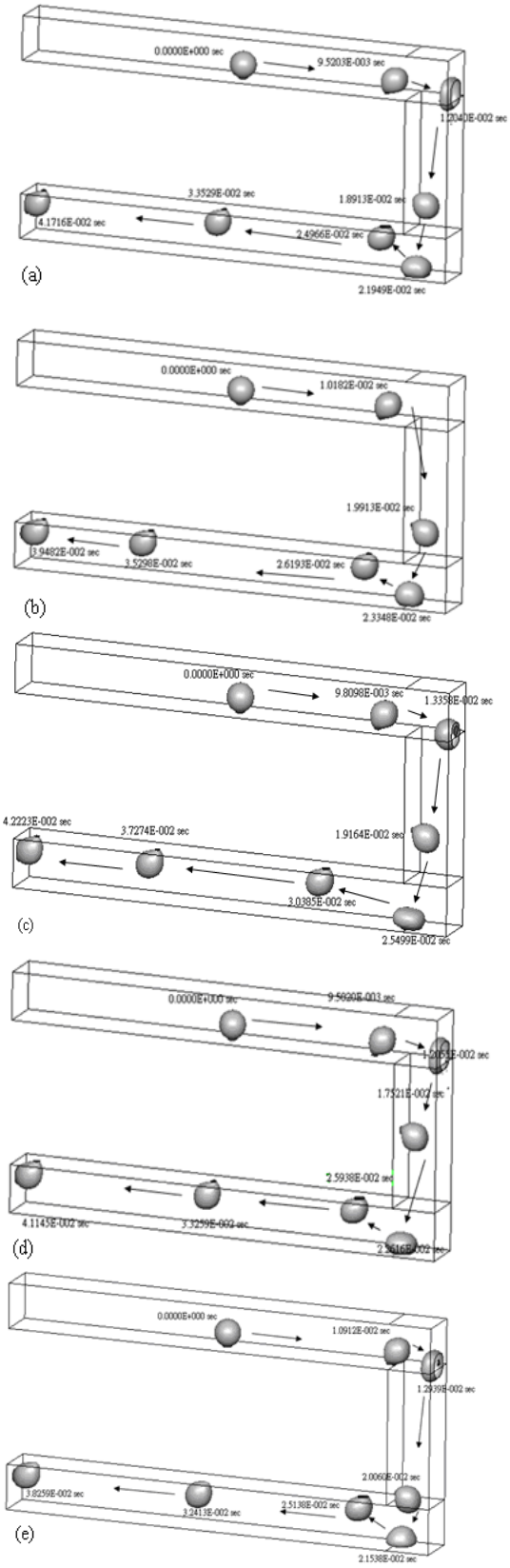

Figure 8 Dynamic behavior of liquid droplet under different gravity directions at V=2 m/s and $\alpha=170°$. (a) x-direction (b) Negative x-direction (c) z-direction (d) y-direction (e) Negative y-direction)

Effects of contact angle

Figure 9 shows the dynamic behavior of the liquid droplets with different contact angles, at V= 2 m/s. The gravity direction is in the negative y-direction. It is found that as contact angle is 70^o, the liquid droplet is very difficult to be moved by the air flow. No appreciable distance the droplet is moved in 9.6×10^{-2} s. Nevertheless, when the contact angle becomes higher, the liquid droplet is easier to be moved. As the contact angle is elevated to 170^o, the droplet is removed from the channel in 3.82×10^{-2} s, as already discussed in Fig. 8. It is found that the water removal velocity increases with the contact angle. For example, as contact angle is assigned to be 70^o, water removal velocity is 0 mm/s; for contact angle of 90^o, water removal velocity is 17.985 mm/s; for contact angle of 120^o, water removal velocity is increased to be 31.685 mm/s.

Table 1 shows the predicted removability of the liquid water droplet on the wall at different contact angle and incoming air velocity. In this table, the symbol "O" denotes the case with removable droplet and "X" is for the non-removable. It is noted that at $\alpha=170^o$, all air velocities can remove the liquid droplets, whereas at $\alpha=70^o$, only the air velocity higher than 5 m/s can remove the liquid droplets.

Experiments have also been conducted to partly demonstrate the numerical predictions. A CCD camera which can take thirty photos per second is used to record the droplet removal process. The serpentine channels are exactly the same as the numerical module, which are 1 mm wide and 1 mm deep. The incoming air velocity is controlled by using an air flow meter. In the experiments, the contact angle of the liquid water droplet is measured to be 70^o. Thus, one may have a chance to compare the numerical and the experimental data for the cases with V=1, 2, 5, and 10 m/s at $\alpha=70^o$. The results are presented in Table 1 and Figure 10. It is shown in Table 1 that the two sets of data regarding the removability of the liquid droplet at $\alpha=70^o$ are in agreement.

In accordance with the data presented in Figs. 9 and 10 and Table 1, it may be concluded that an increase in the contact angle will be very helpful for water removal process. As stated earlier, the contact angle of the liquid water droplets attached on the wall of a metallic bipolar plate can be greatly altered by coating a microscale carbon thin film on the wall. This seemingly appears to be worthy of further study since the contact angle is critical to the liquid droplets removal.

CONCLUDING REMARKS

In this study a numerical simulation based on computational fluid dynamic analysis has been performed toward understanding of the dynamic behavior of the liquid water droplets attached on the channel walls of the bipolar plate of the PEM fuel cell in the water removal process, i The effects of the contact angle is of major concerns, which is varied from 60° to 170°. In addition, the effects of the incoming air velocity and the orientation of the bipolar plate are also regarded as important parameters.

Results show that an appreciable pressure drop is observed over the liquid drop due to the sudden passage contraction caused by the existence of the liquid droplet. It is the difference in pressure between the front and the back of the liquid droplet that produces a form drag to remove the liquid droplet. The pressure difference increases with the size of the liquid droplet.

It is found that at $\alpha=170°$, the liquid droplet can be removed by the air flow even at V=1 m/s. However, at $\alpha=70°$, only the air velocity higher than 5 m/s can remove the liquid droplets. The size of the smaller droplets is a function of the viscosity of the liquid and shear stress interaction between the liquid water and the air stream.

It is noted that the influence of the gravity direction on the dynamic behavior of the liquid droplet is not appreciable. However, the speed of water removal may be affected by changing the gravity direction.

Experiments have also been conducted to demonstrate the numerical predictions to certain extent. The contact angle of the liquid water droplet is measured to be 70^o. Thus, a comparison is made between the numerical and the experimental data for the cases with V=1, 2, 5, and 10 m/s at $\alpha=70^o$. It is observed that the two sets of data regarding the removability of the liquid droplet at $\alpha=70^o$ are in agreement.

ACKNOWLEDGMENT

Authors acknowledge the financial support from Department of Industrial Technology, Ministry of Economic Affairs, Taiwan, under Grant 98-EC-17-A-13-S2-0064.

REFERENCES

[1] H. Li, Y. Tang, Z. Wang a, Z. Shi, S. Wu, D. Song, J. Zhang, K. Fatih, J. Zhang, H. Wang, Z. Liu, R. Abouatallah, A. Mazza, "A review of water flooding issues in the proton exchange membrane fuel cell," Journal of Power Sources 178 (2008) 103.

[2] K. Jiao, B. Zhou, "Innovative gas diffusion layers and their water removal characteristics in PEM fuel cell cathode," Journal of Power Sources 169 (2007) 296.

[3] T.V. Nguyen , "Porton Exchange Membrane Fuel Cells 3," (2006) 1171.

[4] A. D. Le, B. Zhou, " Fundamental understanding of liquid water effects on the performance of a PEMFC with serpentine-parallel channels," Electrochimica Acta 54 (2009) 2137.

[5] C. Song, Y. Tang, J.L. Zhang, J. Zhang, H.Wang, J. Shen, S. McDermid, J. Li, P. Kozak, "PEM fuel cell reaction kinetics in the temperature range of 23-120 degrees,"

Electrochim. Acta 52 (2007) 2552.
[6] J.S. Yi, J. Deliang Yang, C. King, AIChE J. “Water Management along the Flow Channels of PEM Fuel Cells,” Wiley InterScience 50 (2004) 2594.
[7] K. Jiao, B. Zhou, “Effects of electrode wettabilities on liquid water behaviours in PEM fuel cell cathode,” Journal of Power Sources, 175 (2008) 106.
[8] T.F. Fuller, J. Newman, J. Electrochem. “Water and thermal management in solid-polymer-electrolyte fuel cells,” Soc. 140 (1993) 1218.
[9] M.C. Kimble, N.E. Vanderborgh, Proceedings of the 25th Interso-ciety Energy Conversion Engineering Conference, Vol. 3, 1992, p.413.
[10] P. Quan, B. Zhou, A. Sobiesiak, Z. Liu, “Water behavior in serpentine micro-channel for proton exchange membrane fuel cell cathode,” Journal of Power Sources 152 (2005) 131.

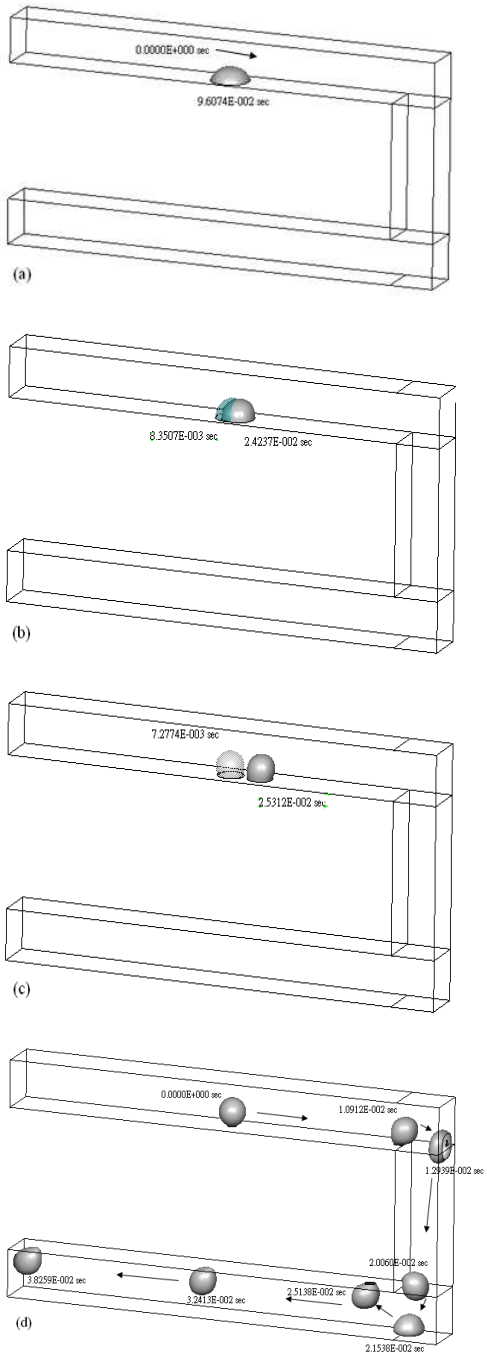

Figure 9 Effects of contact angle on the removability of the liquid droplet at V=2 m/s. The gravity direction is in the negative y-direction.
(a) $\alpha=60^{o}$ (b) $\alpha=90^{o}$ (c) $\alpha=120^{o}$ (d) $\alpha=170^{o}$

Table 1 Removability of liquid water droplet on metallic bipolar plate surface at different contact angle and incoming air velocity.

V (m/s)	Experimental	Numerical			
	α=70°	α=70°	α=90°	α=120°	α=170°
1	X	X	X	O	O
2	X	X	O	O	O
5	O	O	O	O	O
10	O	O	O	O	O

"O" = Removable; "X"=Non-removable

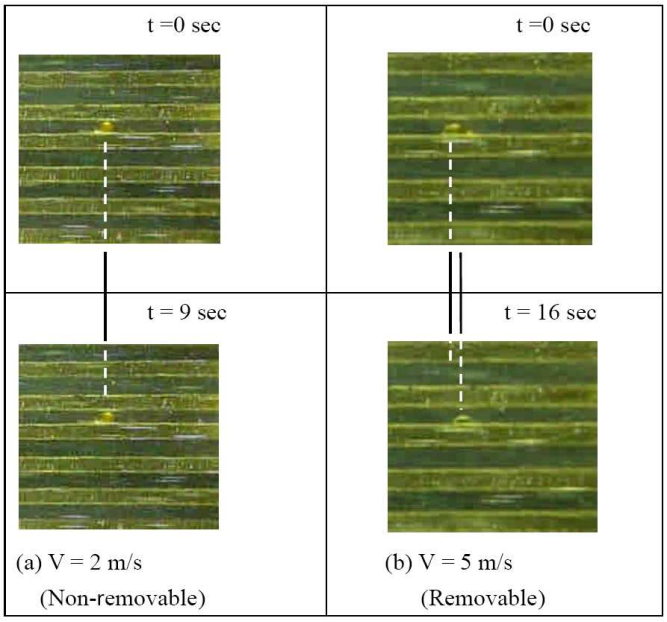

Figure 10 Photos of the liquid droplets, at $\alpha=70^{o}$ and V=2 and 5 m/s. The gravity direction is in the negative y-direction.